Chapter 14
Soft Chemical Ionization Mass Spectrometric Analyses of Hazardous Gases and Decomposition Products of Explosives in Air

Kseniya Dryahina and Patrik Spanel

Abstract The need for rapid and accurate measurement of trace concentrations of compounds present in ambient humid air has led to construction of specialised mass spectrometers based on the Selected Ion Flow Tube Mass Spectrometry, SIFT-MS, its drift-tube variant, SIFDT-MS, and Proton Transfer Mass Spectrometry, PTR-MS. It is currently possible to analyse vapours of volatile organic compounds, VOC, and other gases including ammonia, hydrogen sulphide and hydrogen cyanide present in concentrations even below a part per billion by volume, ppbv. The reagent ions are formed in electrical discharges and their ion-molecule reactions with sampled analyte molecules take place at pressures of 1–2 mbar. As an example of analytical use, SIFT-MS coupled with the Laser Induced Breakdown, LIB, technique was used to analyse stable gaseous products from the decomposition of pure explosive compounds HMX, RDX, PETN and TNT and from 38 types of commercial explosive and propellant mixtures. Decomposition products analysed included NH_3, HCN, HCHO, NO, NO_2, HONO, HNO_3, C_2H_5OH, CH_3CN, DMNB, C_2H_6CO, C_2H_2 and nitroglycerine. For four selected explosives, it was found that the end products of the microscopic LIB laboratory tests correspond well to the composition of fumes from realistic explosions of 0.5 kg charges.

14.1 Introduction

The techniques currently available for analyses of trace gases and volatile organic compound (VOC) vapours in air and breath can be categorised thus:

K. Dryahina (✉) · P. Spanel
Department of Chemistry of Ions in Gaseous Phase, J. Heyrovský Institute of Physical Chemistry of the CAS, Prague, Czech Republic
e-mail: kseniya.dryahina@jh-inst.cas.cz; patrik.spanel@jh-inst.cas.cz

M. F. Pereira, A. Apostolakis (eds.), *Terahertz (THz), Mid Infrared (MIR) and Near Infrared (NIR) Technologies for Protection of Critical Infrastructures Against Explosives and CBRN*, NATO Science for Peace and Security Series B: Physics and Biophysics, https://doi.org/10.1007/978-94-024-2082-1_14

- Spectroscopy (including infrared and terahertz)
- Sensors (including electrochemical, nanoparticle, quartz microbalances)
- Ionization - mass spectrometry (MS) [1], and ion mobility spectrometry (IMS) [2, 3]

MS methods offer superior identification of VOCs and can attain excellent limits of detection, whilst IMS devices often do not need vacuum pumps and can be miniaturised.

The background and state-of-the art of trace gas analysis in breath and environmental monitoring has been reviewed in detail [4–6]. The techniques based on chemical ionization in flow or drift tubes are Selected Ion Flow Tube Mass Spectrometry (SIFT-MS), its drift-tube variant (SIFDT-MS) and Proton Transfer Mass Spectrometry (PTR-MS). They are all based on chemical ionisation by externally generated reagent ions and achieve reliable quantification in defined reaction times. Other relevant and presently available techniques are Secondary Electrospray Ionisation Mass Spectrometry (SESI-MS) [7], which has exceptional sensitivity [8], and the Ion Mobility Spectrometry (IMS) family of techniques that allow selection of ions in handheld instruments [9].

SIFT-MS is used for real-time detection of fumigants, toxic industrial compounds and other hazardous substances at the point of container inspection. Industry-leading accuracy, speed, and reliability for critical safety testing of trapped air in shipping containers is achieved. Mass spectrometric methods based on soft chemical ionisation have been tested for the rapid and simple identification of unknown explosives by controlled decomposition of their trace amounts and subsequent characterization of appropriate spectra of their combustion products. The chemical composition of the headspace and combustion products of the explosives have been analysed by SIFT-MS.

An understanding of the complex processes involved in the decomposition of energetic materials is essential for the development of reliable models for the performance, stability and hazard analysis of explosives. Identification of the decomposition products is of prime importance in identifying toxic, hazardous and environmentally polluting species. Energetic and explosive materials are substances or mixtures that chemically react releasing large amounts of rapidly liberated heat and gases. Today, approximately 150 different formulas are used for the military, commercial, and illicit production of explosives [10, 11]. Energetic materials and explosives may be inorganic or organic in nature and can be divided into two broad categories (low-energy explosives and high-energy explosives) based on how readily a reaction is initiated and its intensity.

Most trace explosive detection techniques, such as IMS and gas chromatography (GC), rely on vapour detection. Unfortunately, at room temperature, the vapour pressures of many common explosives are extremely small (ppbv or less), and attempts to conceal the explosives by sealing them in packaging materials can decrease the vapour concentrations by as many as three orders of magnitude [12]. An alternative optical technique for the detection of explosives is laser-induced breakdown spectroscopy (LIBS) [13]. The ability of LIBS to provide a remote, rapid

multi-element microanalysis of bulk samples (solid, liquid, gas and aerosol) in the parts-per-million by volume, ppmv, range with little or no sample preparation has been widely demonstrated and it is the greatest advantage of LIBS compared with other analytical approaches. LIBS holds particular promise for the detection and identification of explosives because of its intrinsic capability for minimally destructive, in situ, real-time detection and analysis of chemical species. More recently, the capability of LIBS to identify compounds has been realised with the advent of high-resolution broadband spectrometers. A promising method for the analysis of the stable decomposition products of energetic materials is a combination of LIB with SIFT-MS. [12, 14–16]

14.2 Quantitative Mass Spectrometry Techniques for Trace Gas Analysis

14.2.1 Selected Ion Flow Tube Mass Spectrometry (SIFT-MS)

Selected ion flow tube mass spectrometry (SIFT-MS) is a quantitative mass spectrometry technique for trace gas analysis which involves the chemical ionization of trace volatile compounds by selected positive reagent ions during a well-defined time period along a flow tube [17–19]. Absolute concentrations of trace compounds present in air, exhaled breath or the headspace of samples can be calculated in real time from the ratio of the reagent and analyte ion signal ratios, without the need for sample preparation or calibration with standard mixtures. H_3O^+, NO^+ and $O_2^{+\bullet}$ are the most suitable reagent ions, because they do not react rapidly with the major components of air and breath viz. N_2, O_2, H_2O, CO_2 and Ar, but they do react rapidly with most VOCs forming characteristic analyte ions that identify the various neutral molecules, M, in the air sample being analysed. However, when humid air or breath is analysed, hydrated ions of the kind $H_3O^+(H_2O)_{1,2,3}$, and $NO^+(H_2O)_{1,2}$ can form from the simple ions and these hydrates can also act as reagent ions leading to hydrated analyte ions of the kind $MH^+(H_2O)_{1,2,3}$. Then it is important to recognise that all the reagent and characteristic analyte ion species must be included to obtain correct analysis of each M [17–19].

A simple example is the reaction of acetone with H_3O^+ reagent ions in SIFT-MS. It proceeds rapidly by the process of proton transfer producing protonated acetone:

$$H_3O^+ + CH_3COCH_3 \rightarrow CH_3COCH_3H^+ + H_2O \qquad (14.1)$$

When the concentration of acetone, [M], is small, the fractional reduction in the large reagent ion count rate is immeasurably small, but the much smaller count rates of the analyte ions can still be determined accurately. It is easy to show that the number density of the analyte ions $[MH^+]$ are related to the number density of the

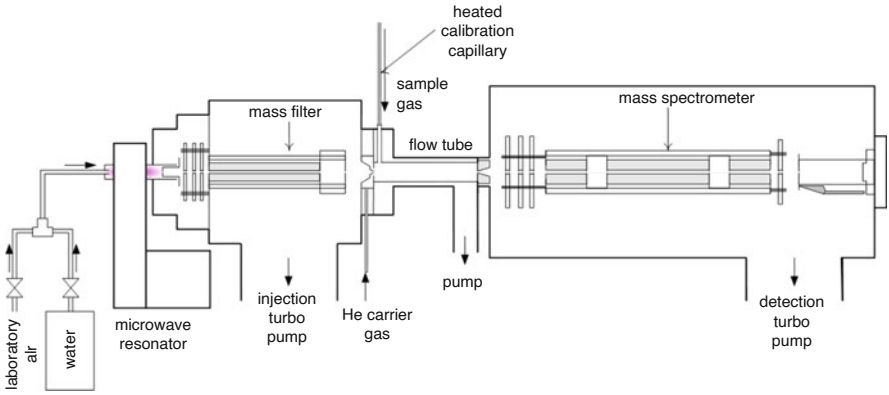

Fig. 14.1 Schematics of the *Profile* 3 SIFT-MS instrument. (Reproduced from Ref. [14] with permission from The Royal Society of Chemistry)

reagent ions $[H_3O^+]$ as $[MH^+] = [H_3O^+]k[M]tD_e$. where k is the rate coefficient for the reaction of the H_3O^+ ions with the trace gas analyte molecules present at a number density [M] and t is the reaction time. D_e is a differential diffusion enhancement coefficient that accounts for the fact that the reagent ions and the analyte ions diffuse at different rates to the walls of the flow tube and this influences their relative number densities at the downstream sampling orifice (see Fig. 14.1), and this differential diffusion must be accounted for to obtain an accurate quantification of M. [18, 20–22] Also, mass discrimination against larger *m/z* ions in the analytical quadrupole mass spectrometer [20, 22] and the formation of hydrated reagent and analyte ions [18, 22] must be accounted for. Thus, the concentrations of trace gases in humid component mixtures such as exhaled breath can readily be calculated from the observed count rates of each analyte ion species. Of great significance is that the analyses only involve the ratio of the characteristic analyte ion count rates to the reagent ion count rates and so any drift in the reagent ion count rate does not invalidate the analyses.

The detection sensitivity of a SIFT-MS instrument depends on the count rates of the reagent ions that can be realised. For the current *Profile 3* instruments [20] these are up to 3 million counts-per-second, c/s, and the sensitivity for most VOCs is typically 10 c/s per ppbv corresponding to a practical detection limit of 1 ppbv per second of integration time. Detection limits in the sub-ppbv range have been validated for aromatic hydrocarbons [23] using longer integration times. The absolute accuracy of SIFT-MS has been validated to be better than 10% [20, 22, 24] for several compounds without the need for external standards, as long as the sample and carrier gas flow rates and flow tube temperature are accurately known and mass discrimination and diffusion effects are accounted for.

SIFT-MS instruments can be operated in two modes: They are (i) the full scan (FS) mode in which a complete mass spectrum of reagent and analyte ions is obtained by sweeping the analytical quadrupole mass spectrometer over a selected *m/z*, range for a chosen time whilst a sample of air or breath is introduced into the

carrier gas. The resulting mass spectrum is interpreted by relating the analyte ions to the trace gases present in the sample using the acquired knowledge of the ion chemistry. The concentrations of the individual trace gases can be calculated using the in-built kinetics library. (ii) the multiple ion monitoring (MIM) mode in which the count rates of the reagent ions and their hydrates, such as $H_3O^+(H_2O)_n$, and a number of characteristic analyte ions appropriate to the number of trace compounds to be analysed are monitored as air or breath displaces the ambient air at the entrance to the sampling capillary (see Fig. 14.1). This reagent ion and analyte ion monitoring is achieved by rapidly switching the downstream mass spectrometer between the several *m/z* values of the reagent and analyte ions, dwelling on each *m/z* for a predetermined short time interval. This real-time monitoring is possible because of the fast time response of SIFT-MS, which is typically less than 20 ms. The humidity of the sampled air (for example, exhaled breath consists of 6% water vapour) is routinely obtained from the data and is an indicator of sample quality and control [25].

14.2.2 Proton Transfer Reactions Mass Spectrometry (PTR-MS)

Proton transfer reactions mass spectrometry (PTR-MS) is essentially a flow-drift tube chemical ionisation (CI) analytical technique [26–28]. Ions are generated in a hollow cathode discharge and injected into a flow-drift tube buffered with the sample gas to be analysed, usually air. The ions experience an electric field coaxial with the flow tube and gain energy reaching a drift speed in the field direction and arrive at a downstream orifice where they are sampled into a differentially pumped mass spectrometer system and analysed in an analogous way to that in SIFT-MS. The reagent ions mostly used to date are H_3O^+ so, as explained previously; the primary reaction process utilized for analysis is proton transfer exemplified by reaction (14.1). Because a mass filter is not used to select reagent ions, higher currents of reagent ions can be injected, and the axial electric field results in less diffusive loss of the reagent ions to the walls of the flow-drift tube. Diffusive loss is also reduced by usage of air (the sample to be analysed) as the buffer/carrier gas rather than the lighter helium gas as used in SIFT-MS. the pressures used in the PTR-MS drift tube being different than that used in SIFT-MS flow tube. The net result is that greater count rates of the reagent H_3O^+ ions are available which leads to greater analytical sensitivity. Thus, detection limits can be in the parts-per-trillion by volume, pptv, to the sub-ppbv regime [29, 30]. Since the reagent ion energies are elevated above thermal, the formation of cluster ions of the kind $H_3O^+(H_2O)_{1,2,3}$ are suppressed in comparison with SIFT-MS, although the actual count rates depend sensitively on the ratio of electric field strength to the buffer gas number density, E/N. A very good review of PTR-MS has been given recently [27].

The kinetics of the analytical ion-molecule reactions and the reaction time can be sensitive to E/N; thus accurate quantification is not simply achieved. A canonical value (2×10^{-9} cm^3s^{-1}) for the collisional reaction rate coefficients, k_c, is often used to estimate trace gas concentrations from PTR-MS data. Quantification is directly dependent on k, which can vary widely for ion-molecule reactions in the thermal energy regime (over the range $1–5 \times 10^{-9}$ cm^3s^{-1}), so a commensurate uncertainty can be introduced into PTR-MS quantification. However, such uncertainties can be minimised using calibration techniques. It is for these reasons that PTR-MS has been used only sporadically for breath analysis [31] where greater accuracy is needed; rather, it has mostly been used for air analysis [28] and environmental studies [32, 33]. A further problem is that following proton transfer from H_3O^+ to M, some MH^+ nascent analyte ions can undergo spontaneous unimolecular dissociation or collision induced dissociation, and this must be recognised to avoid false compound identifications; see for example [34, 35]. Unimolecular dissociation of MH^+ analyte ions can occur even under the thermal energy conditions of SIFT-MS [36–38], but collision induced dissociation is exacerbated in PTR-MS where the ion-molecule interaction energies are suprathermal. Further, in conventional PTR-MS it is also impossible to separate isobaric compounds when only H_3O^+ reagent ions are used, because they simply result in MH^+ ions with the same *m/z* or fragments of these. This problem is alleviated in SIFT-MS that exploits NO^+ and $O_2^{+\bullet}$ reagent ions also. Other reagent ions can be used by changing the discharge gas composition in PTR-SRI-MS instruments [29] and high resolution analytical time-of-flight, TOF, mass spectrometers that can separate nominally isobaric compounds. [39–41]

14.2.3 Selected Ion Flow Drift-Tube Mass Spectrometry (SIFDT-MS)

The selected ion flow drift tube mass spectrometric analytical technique (SIFDT-MS) [42–44] extends the SIFT-MS by the inclusion of a static but variable *E*-field along the axis of the flow tube reactor in which the analytical ion-molecule chemistry occurs (see Fig. 14.2). The ion axial speed is increased in proportion to *E/N*. The residence/reaction time, *t*, measured by Hadamard transform multiplexing, is proportionally reduced. To ensure a proper understanding of the physics and ion chemistry underlying SIFDT-MS, ion diffusive loss to the walls of the flow-drift tube and the mobility of injected H_3O^+ ions have been studied as a function of *E/N* [44]. The production of hydrated reagent and analyte ion also has been experimentally investigated [44].

The analytical performance of SIFDT-MS has been demonstrated by the quantification of acetone and isoprene in exhaled breath. [44] A major advance compared to SIFT-MS is that the speed of ions through the reaction zone can be achieved using the adjustable *E*-field, which allows the suppression of ion diffusion losses even at

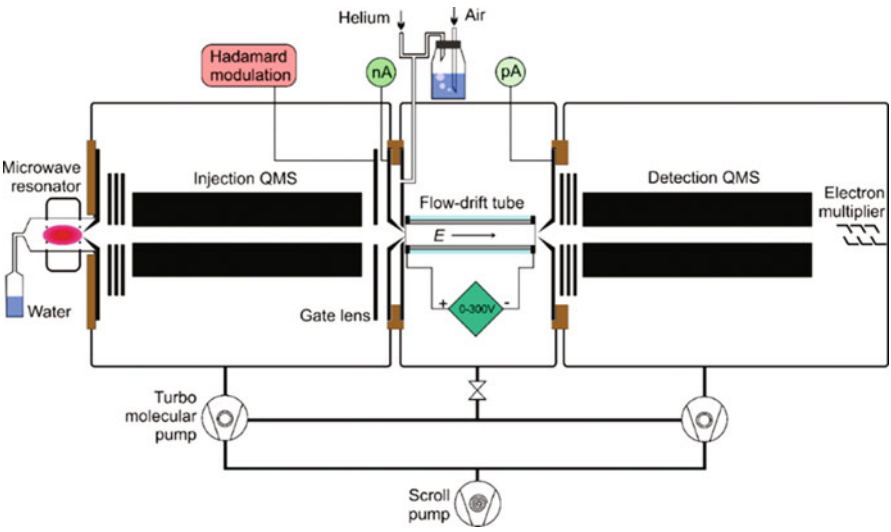

Fig. 14.2 Schematic drawing of the SIFDT apparatus. Note that the flow speed of the helium carrier gas is reduced by a restrictive aperture between the flow-drift tube compartment and the scroll pump. (Reprinted with permission from Ref. [44]. Copyright (2015) American Chemical Society)

very low carrier gas flow speeds. This corresponds to helium carrier gas and sample gas flow rates more than 7 times lower than those used in *Profile 3* SIFT-MS instruments. Thus, a less powerful vacuum pump can be used to maintain the gas flow along the ion-chemical reactor and a smaller helium carrier gas pressure reservoir is needed, which facilitates production of smaller and more versatile transportable instruments. Furthermore, smaller sample flow rates can be used for analysis, which is a distinct advantage when liquid headspace is to be analysed, which results in the less formation of ion hydrates. The simplicity of construction of the SIFDT-MS instrument is due to the use of a resistive glass flow-drift tube element and by adopting the Hadamard transform multiplexing for direct reaction time measurement, which is another improvement on SIFT-MS in which the reaction times are fixed and calculated indirectly from the carrier gas pressure and flow rate. The presence of the *E*-field results in an increase of the kinetic and internal energies of the ions that influences hydrated ion formation. Initial studies have confirmed that variation of *E/N* modifies the count rates of hydrated analyte ions relatively to the primary analyte ions without significantly modifying the bimolecular ion chemistry [42], thus promising more accurate analyses. However, it is worthy of note that increasing *E/N* to higher values (>20 Td) can promote controlled collisional dissociation of ions, and this might ultimately allow isobaric ions to be distinguished, a technique well known in MS-MS methods.

14.3 Decomposition Products of Explosives

To study degradation products of explosives material, SIFT-MS has been coupled with LIB. Thus, a small amount of a sample was irradiated by a sequence of 10 laser pulses each of 150 mJ using an ArF excimer laser and the stable gaseous products from the reaction zone were analysed simultaneously using SIFT-MS (see Fig. 14.3). More than 40 types of commercially produced explosives and propellants were studied in this experimental set-up and a spectral database was obtained. The concentrations of the decomposition products were determined for pure explosive compounds like HMX, RDX, PETN and TNT and for 38 types of commercially produced explosives and propellants.

Four typical representatives of industrial explosives were chosen also for the analyses of fumes from realistic explosions:

- EMSIT 1 is the underground blasting explosive of emulsion type based on ammonium and sodium nitrates;
- Ostravit C is a semi-plastic permissible gas-proof explosive contains nitro esters, mixture of nitroglycerine and ethylene glycol dinitrate;
- Perunit 28E is an explosive of a classical dynamite type; is a mixture of ammonium nitrate, nitrocellulose, and nitroglyceroglycol;
- Permonex V19 is the underground blasting powder explosive based on ammonium nitrate and TNT.

Analyses involving these explosives were carried out in four different ways:

- volatile compounds released into the **headspace** of explosives were sampled from 40 mL vials with small amount of explosive (5 g) without initiating breakdown or explosion.

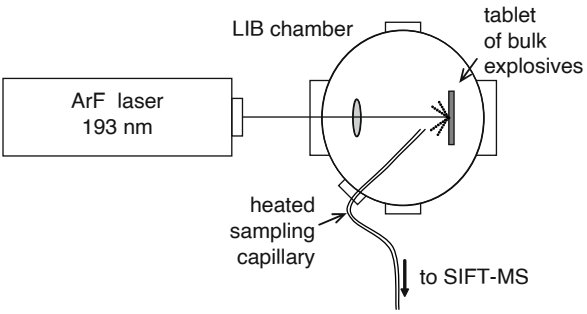

Fig. 14.3 Schematic diagram of the experimental apparatus. An ArF excimer laser (193 nm, 20 ns, and 150 mJ) was used to create pulses of radiation that were focused by a 15 cm quartz lens onto the surface of a rotating target placed in a vacuum chamber filled with Ar at a pressure of 1 atm. The stable gaseous products originating from the plasma generated by ten repeated laser pulses were extracted via a heated calibrated PEEK capillary. (Reproduced from Ref. [14] with permission from The Royal Society of Chemistry)

- fumes after **detonation** of 500 g of each explosive in a test tunnel collected into 2 L glass vessels.
- headspace above 1 kg of **sand** collected after explosion of 50 g of explosives in a steel barrel containing 10 kg of clean dry sand.
- fumes from the reaction zone of the **LIB** chamber in real time by SIFT-MS; a sequence of 10 laser pulses, 150 mJ each (ArF excimer laser) was used to simulate the explosion or combustion on a microscopic laboratory scale. The experimental set-up is shown in Fig. 14.3

SIFT-MS spectra were collected in the full scan mode over the range of *m/z* 10–240 which fully covers the generated volatiles at room temperature. The spectra obtained for Perunit 28E explosive are shown in Fig. 14.4. The composition of the end products of laser generated plasma plumes corresponds well to the composition of fumes collected after explosion of a much larger (500 g) charges.

HCN is a typical analyte of the explosion and it is not present in the headspace of any of the explosives. It is not surprising that it is present in the LIB samples and in the fumes after explosion in a test tunnel. However, we did not expect to see such a relatively large amount of HCN in sand samples. In order to confirm that HCN is generated in the LIB plume chemistry, the MIM mode of the SIFT-MS instrument was used to record time profiles of the concentrations of HCN during and after repeated LIB events. The plot of the real time variation of concentration of HCN in response to two separate laser pulses is shown in Fig. 14.5. HCN is generated immediately after the laser pulse and its concentration then slowly decreases over several seconds due to its diffusion into the volume of the experimental chamber.

The exponential time constant for the decay of 15 s corresponds to a characteristic diffusion length of 3–4 cm considering a diffusion coefficient 0.2 $cm^2\ s^{-1}$. Part of HCN is produced by the reaction of excited CN radicals with water vapor molecules H_2O [14]. The activation energy of this reaction is 4.7 kcal mol^{-1} [14] and this reaction is thus easily energetically accessible at $T > 4000$ K. The concentrations obtained using the same experimental apparatus in the absence of any explosive samples are also given. Note that the levels of ethanol, NO, NO_2, HONO, and HCN were significantly elevated in all of the LIB experiments [12].

The concentrations of the decomposition products (NH_3, HCN, HCHO, NO, NO_2, HONO, HNO_3, C_2H_5OH, CH_3CN, DMNB, C_2H_6CO, C_2H_2 and nitroglycerine) were determined for pure explosive compounds HMX, RDX, PETN and TNT [14, 16] and for commercially produced explosives and propellants [12, 15]. The mean absolute concentrations of these stable products obtained during the first 10 s after the LIB event for the several explosives are given in Table 14.1 in units of ppbv, equivalent to nmol mol^{-1}. Trace amounts of DMNB were present due to its use as a volatile marker deliberately added into some explosives in the manufacturing process.

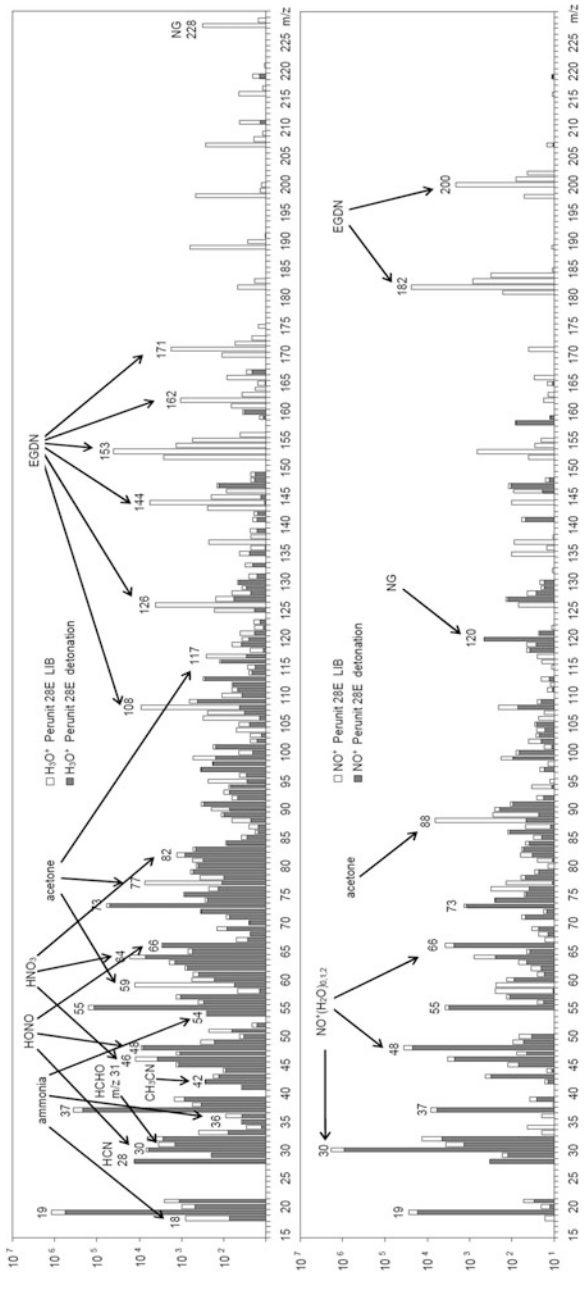

Fig. 14.4 Comparison of SIFT-MS spectra of the fumes after detonation in a test tunnel with the spectra of the fumes obtained on a microscopic scale by the LIB method is presented for Perunit 28E

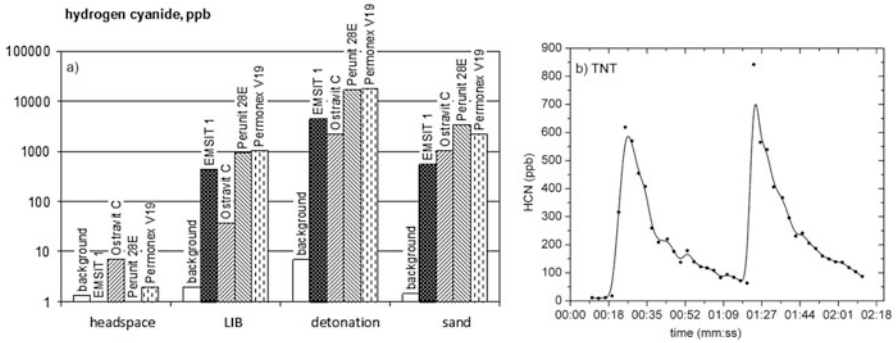

Fig. 14.5 (**a**) HCN concentration in ppb unit quantified in the headspace and fumes after detonation in test tunnel (detonation) and after combustion on a microscopic laboratory scale (LIB), headspace above sand collected after explosion. (**b**) Time dependence of the HCN concentration obtained by SIFT-MS after irradiation of a TNT sample by two sequential laser pulses. (Reproduced from Ref. [14] with permission from The Royal Society of Chemistry)

14.4 Conclusions

The combined experiments using LIB and SIFT-MS have allowed the analyses of the volatile decomposition products of commercial explosive mixtures, and it has been demonstrated that the methodology presented in this paper can be used for safe and non-destructive studies of characteristic explosion products without the need for the initiation of hazardous quantities of explosives in the form of test charges. It is also interesting to note that according to preliminary experiments, the compositions of the end products of the laser-generated plasma plumes correspond well to the composition of the fumes collected after the explosion of much larger (0.5 kg) charges. Therefore, we suggest that the results of the present study are relevant to the analysis of gaseous residues of explosions and the combustion products of real explosives and propellants.

Before concluding we would like to mention that materials [45, 46] and compact devices such as quantum cascade lasers and superlattice multipliers [47–52] are under development for the GHz-THz-MIR range, where the substances analysed here have well defined absorption signatures. These devices can deliver complementary sensors that can be combined with those here. A joint effort can potentially increase the efficiency for detection of hazardous gases and decomposition products of explosives in air.

Table 14.1 Mean concentrations in parts per billion by volume (ppbv) of the compounds identified by SIFT-MS in the atmosphere inside the experimental chamber after the initiation of the explosive samples using laser pulses

Sample	Acetylene	Acetonitrile	Ammonia	DMNB	Formaldehyde	Hydrogen cyanide	Nitric acid	Nitric oxide	Nitrous acid	Nitrogen dioxide	Nitroglycerine
TNT	28	4	46	32	46	533	75	339	45	171	4
RDX	3	8	56	9	87	746	58	856	48	90	0
HMX	0	0	10	17	11	18	22	462	38	163	6
PETN	13	10	19	18	285	91	21	1129	41	221	0
EMSIT 1	127	8	502	11	437	448	159	2144	932	2831	20
Ostravit C	9	0	1872	30	498	84	524	2218	1275	5786	242
Perunit 28E	46	8	287	21	1508	801	17,832	19,694	3094	64,513	355
Permonex V19	0	0	19	0	4	12	6	112	8	69	0
Guanidinium nitrate	0	1	21	8	39	11	30	553	25	18	2
Nitrosourea	0	0	8	0	23	6	16	572	8	30	2
Urea nitrate	0	0	14	4	38	9	33	255	17	30	1
Pickric acid	0	0	17	3	30	8	15	548	6	34	2
Tetryl	6	1	29	3	38	57	24	907	15	62	3
Ammonium nitrate	0	1	37	2	44	5	14	861	16	59	1
Semtex 10	0	3	15	72	117	116	75	479	29	28	6
Semtex 1A	103	3	70	62	132	101	62	767	31	87	0
PETN+wax	29	3	45	11	82	47	27	1009	23	89	1
Nitrocelullose A	0	0	47	3	113	32	36	580	50	64	0
Nitrocelullose B	2	0	40	2	89	15	44	565	85	43	2
Lovex S011	0	0	30	6	121	3	46	343	19	37	2
Lovex S040	0	0	24	10	150	23	52	765	34	146	3

Data from Refs. [15, 16]

References

1. Pu F et al (2019) Direct sampling mass spectrometry for clinical analysis. Analyst 144:1034–1051
2. Covington JA et al (2015) The application of FAIMS gas analysis in medical diagnostics. Analyst 14:6775–6781
3. Baumbach JI (2009) Ion mobility spectrometry coupled with multi-capillary columns for metabolic profiling of human breath. J Breath Res 3:034001
4. Davies SJ et al (2014) Breath analysis of ammonia, volatile organic compounds and deuterated water vapor in chronic kidney disease and during dialysis. Bioanalysis 6:843–857
5. Španěl P, Smith D (2011) Volatile compounds in health and disease. Curr Opin Clin Nutr Metab Care 14:455–460
6. Finamore P et al (2019) Breath analysis in respiratory diseases: state-of-the-art and future perspectives. Expert Rev Mol Diagn 19:47–61
7. Garcia-Gomez D et al (2016) Secondary electrospray ionization coupled to high-resolution mass spectrometry reveals tryptophan pathway metabolites in exhaled human breath. Chem Commun 52:8526–8528
8. Ke MF et al (2019) Generating supercharged protein ions for breath analysis by extractive electrospray ionization mass spectrometry. Anal Chem 91:3215–3220
9. Anttalainen O et al (2018) Differential mobility spectrometers with tuneable separation voltage - theoretical models and experimental findings. Trac-Trends Anal Chem 105:413–423
10. Matyáš R, Pachman J (2013) Primary explosives. Springer, Berlin/Heidelberg
11. Politzer P, Murray JS (2003) Energetic materials. Part 2. Detonation, combustion. Elsevier Science, Amsterdam
12. Civiš M et al (2011) Laser ablation of FOX-7: proposed mechanism of decomposition. Anal Chem 83:1069–1077
13. Cremers DA, Radziemski LJ (2013) Handbook of laser-induced breakdown spectroscopy, 2nd edn. Blackwell Science Publishing, Oxford
14. Sovová K et al (2010) A study of the composition of the products of laser-induced breakdown of hexogen, octogen, pentrite and trinitrotoluene using selected ion flow tube mass spectrometry and UV-Vis spectrometry. Analyst:1106–1114
15. Civis S et al (2016) Selected ion flow tube mass spectrometry analyses of laser decomposition products of a range of explosives and ballistic propellants. Anal Methods 8:1145–1150
16. Lehký L, Kyncl M (2008) Projekt report. FT-TA4/124: research of new methods of detection of explosives
17. Španěl P, Smith D (1996) Selected ion flow tube: a technique for quantitative trace gas analysis of air and breath. Med Biol Eng Comput 34:409–419
18. Španěl P et al (2006) A general method for the calculation of absolute trace gas concentrations in air and breath from selected ion flow tube mass spectrometry data. Int J Mass Spectrom 249:230–239
19. Smith D, Španěl P (2005) Selected ion flow tube mass spectrometry (SIFT-MS) for on-line trace gas analysis. Mass Spectrom Rev 24:661–700
20. Smith D et al (2009) Ionic diffusion and mass discrimination effects in the new generation of short flow tube SIFT-MS instruments. Int J Mass Spectrom 281:15–23
21. Dryahina K, Španěl P (2005) A convenient method for calculation of ionic diffusion coefficients for accurate selected ion flow tube mass spectrometry, SIFT-MS. Int J Mass Spectrom 244:148–154
22. Španěl P, Smith D (2001) Quantitative selected ion flow tube mass spectrometry: the influence of ionic diffusion and mass discrimination. J Am Soc Mass Spectrom 12:863–872
23. Dryahina K et al (2018) Quantification of volatile compounds released by roasted coffee by selected ion flow tube mass spectrometry. Rapid Commun Mass Spectrom 32:739–750
24. Španěl P et al (1997) Validation of the SIFT technique for trace gas analysis of breath using the syringe injection technique. Ann Occup Hyg 41:373–382

25. Španěl P, Smith D (2001) On-line measurement of the absolute humidity of air, breath and liquid headspace samples by selected ion flow tube mass spectrometry. Rapid Commun Mass Spectrom 15:563–569
26. Lindinger W et al (1998) On-line monitoring of volatile organic compounds at pptv levels by means of proton-transfer-reaction mass spectrometry (PTR-MS) medical applications, food control and environmental research. Int J Mass Spectrom Ion Process 173:191–241
27. Blake RS et al (2009) Proton-transfer reaction mass spectrometry. Chem Rev 109:861–896
28. J d G, Warneke C (2007) Measurements of volatile organic compounds in the earth's atmosphere using proton-transfer-reaction mass spectrometry. Mass Spectrom Rev 26:223–257
29. Jordan A et al (2009) An online ultra-high sensitivity proton-transfer-reaction mass-spectrometer combined with switchable reagent ion capability (PTR+ SRI- MS). Int J Mass Spectrom 286:32–38
30. Lindinger W, Jordan A (1998) Proton-transfer-reaction mass spectrometry (PTR-MS): on-line monitoring of volatile organic compounds at pptv levels. Chem Soc Rev 27:347–375
31. Karl T et al (2001) Human breath isoprene and its relation to blood cholesterol levels: new measurements and modeling. J Appl Physiol 91:762
32. De Gouw J et al (2003) Validation of proton transfer reaction-mass spectrometry (PTR-MS) measurements of gas-phase organic compounds in the atmosphere during the New England Air Quality Study (NEAQS) in 2002. J Geophys Res-Atmos 108(4682)
33. Hewitt C et al (2003) The application of proton transfer reaction-mass spectrometry (PTR-MS) to the monitoring and analysis of volatile organic compounds in the atmosphere. J Environ Monit 5:1–7
34. Taipale R et al (2008) Technical note: quantitative long-term measurements of VOC concentrations by PTR-MS-measurement, calibration, and volume mixing ratio calculation methods. Atmos. Chem Phys 8:6681–6698
35. Schripp T et al (2010) Interferences in the determination of formaldehyde via PTR-MS: what do we learn from m/z 31? Int J Mass Spectrom 289:170–172
36. Schoon N et al (2007) A selected ion flow tube study of the reactions of H_3O^+, NO^+ and O_2^+ with a series of C_5, C_6 and C_8 unsaturated biogenic alcohols. Int J Mass Spectrom 263:127–136
37. Španěl P et al (2004) Quantification of hydrogen cyanide in humid air by selected ion flow tube mass spectrometry. Rapid Commun Mass Spectrom 18:1869–1873
38. Dhooghe F et al (2009) Flowing afterglow selected ion flow tube (FA-SIFT) study of ion/molecule reactions in support of the detection of biogenic alcohols by medium-pressure chemical ionization mass spectrometry techniques. Int J Mass Spectrom 285:31–41
39. Blake RS et al (2006) Chemical ionization reaction time-of-flight mass spectrometry: multi-reagent analysis for determination of trace gas composition. Int J Mass Spectrom 254:85–93
40. Wyche K et al (2005) Differentiation of isobaric compounds using chemical ionization reaction mass spectrometry. Rapid Commun Mass Spectrom 19:3356–3362
41. Blake R et al (2004) Demonstration of proton-transfer reaction time-of-flight mass spectrometry for real-time analysis of trace volatile organic compounds. Anal Chem 76:3841–3845
42. Spesyvyi A et al (2017) Ion chemistry at elevated ion-molecule interaction energies in a selected ion flow-drift tube: reactions of H_3O^+, NO^+ and O_2^+ with saturated aliphatic ketones. Phys Chem Chem Phys 19:31714–31723
43. Spesyvyi A et al (2016) In-tube collision-induced dissociation for selected ion flow-drift tube mass spectrometry, SIFDT-MS: a case study of NO+ reactions with isomeric monoterpenes. Rapid Commun Mass Spectrom 30:2009–2016
44. Spesyvyi A et al (2015) Selected ion flow-drift tube mass spectrometry: quantification of volatile compounds in air and breath. Anal Chem 87:12151–12160
45. Oriaku CI, Pereira MF (2017) Analytical solutions for semiconductor luminescence including coulomb correlations with applications to dilute bismides. J Opt Soc Am B 34:321–328
46. Pereira MF (2017) Analytical expressions for numerical characterization of semiconductors per comparison with luminescence. Materials (Basel) 11:2

47. Pereira MF (2016) The linewidth enhancement factor of intersubband lasers: from a two-level limit to gain without inversion conditions. Appl Phys Lett 109:222102
48. Pereira MF et al (2017) Terahertz generation by gigahertz multiplication in superlattices. J Nanophoton 11(046022)
49. Apostolakis A, Pereira MF (2019) Controlling the harmonic conversion efficiency in semiconductor superlattices by interface roughness design. AIP Adv 9:015022
50. Apostolakis A, Pereira M (2019) Potential and limits of superlattice multipliers coupled to different input power sources. J Nanophoton 13:036017
51. Apostolakis A, Pereira MF (2020) Superlattice nonlinearities for gigahertz-terahertz generation in harmonic multipliers. Nano 9(12):3941–3952. https://doi.org/10.1515/nanoph-2020-0155
52. Pereira MF, Anfertev V, Shevchenko Y, Vaks V (2020) Giant controllable gigahertz to terahertz nonlinearities in superlattices. Sci Rep 10:15950